Prenatal opioid exposure inhibits microglial sculpting of the dopamine system during adolescence

Caroline J. Smith*[2], Tania Lintz*[1], Madeline Clark[2], Karen E. Malacon[2], Nicholas Constantino[1], Alia Abiad[1], Yanaira Alonso-Caraballo[1,], Veronica Kim[2], Young C. Jo[2], Staci D. Bilbo*[2], Elena H. Chartoff*[1]

1. Mclean Hospital, Harvard Medical School, Belmont, MA
2. Duke University, Durham, NC

*These authors contributed equally

Abstract

The current opioid epidemic has dramatically increased the number of children who are prenatally exposed to opioids, including oxycodone. However, little is know about the mechanisms by which prenatal opioid exposure leads to long term changes in reward circuit function and behavior. Microglia, the resident immune cells of the brain, are known to respond to perinatal opioid exposure and to sculpt neural circuits during development. Indeed, we recently found that microglial phagocytosis of dopamine D1 receptors in the nucleus accumbens (NAc) is required for the natural developmental decline in NAc-D1R that occurs between adolescence and adulthood. Morever, this microglial pruning occurs only in males, and is required for the normal developmental trajectory of social play behavior. Here, we show that maternal oxycodone self-administration during pregnancy leads to higher D1R density within the NAc in adult male, but not female, offspring in rats. Furthermore, adolescent microglial phagocytosis of D1R is reduced following prenatal oxycodone exposure. This work demonstrates for the first time that microglia play a key role in translating prenatal opioid exposure to long-term changes in neural systems.

Highlights

- Prenatal opioid exposure decreases offspring body weight in males and females
- Prenatal opioid exposure does not alter D2 receptor or Tyrosine Hydroxylase fiber density in either sex
- Prenatal opioid exposure increases nucleus accumbens dopamine D1 receptor expression in males but not females
- Prenatal opioid exposure decreases microglial phagocytosis of D1R in the nucleus accumbens in males only

Keywords: Microglia, dopamine, phagocytosis, prenatal opioid, oxycodone, nucleus accumbens

Introduction

In the past decade, rates of opioid use disorder have increased to epidemic proportions (Haight et al., 2018). This includes a dramatic increase in disorders among pregnant mothers, and therefore the incidence of prenatal exposure in their children. Indeed, the Centers for Disease Control and Prevention report that between 1999 and 2014 the incidence of opioid use disorder at delivery increased by 333% (Haight et al., 2018). Infants exposed to opioids during gestation often develop neonatal opioid withdrawal syndrome (NOWS) which is characterized by tremors, difficulty feeding, high-pitched crying, inconsolability, and diarrhea (Conradt et al., 2019; Arter et al., 2021). While these symptoms can be acutely managed with opioid replacement therapies, very little is known about the long-term consequences of prenatal opioid exposure for brain development and behavior.

The existing literature on the long-term effects of prenatal opioid exposure, while sparse, points towards enduring consequences. For example, differences have been found between school age children exposed to opioids in utero and un-exposed children in intelligence quotient (IQ)/cognitive performance (Nygaard et al., 2015; van Baar et al., 1994), visual acuity (Moe, 2002), language (Hunt et al., 2008; Benninger et al., 2020), attention-deficit disorder and/or hyperactivity (Sandtorv et al., 2018), and aggression and anxiety (de Cubas & Field, 1993). Nygaard et al. (2017) found that 17–to-21-year-olds prenatally exposed to opioids scored significantly lower on a number of cognitive performance metrics as compared to un-exposed peers. Importantly, however, interpretation of the human literature is confounded by several factors, including retrospective chart review, small sample sizes, and variables such as maternal nutrition, access to health care, socio-economic status, and maternal mental health (Singer et al., 2020; Conradt et al., 2019). Interestingly, Nygaard et al. (2015), using a prospective study design, found that boys, but not girls, exposed to opioids in utero had lower IQ scores at 8 years of age. Similarly, boys, but not girls, have poorer language and cognitive scores following prenatal opioid exposure during early childhood (Skumlien et al., 2020). These findings suggest the potential for a male bias in susceptibility to the long-term effects of prenatal opioid exposure.

A wide array of behavioral and neurobiological changes have also been identified in animal models of prenatal opioid exposure (for review see Byrnes & Vassoler, 2018; Abu & Roy, 2021, Boggess & Risher, 2020). For example, adult male rats exposed to morphine during gestation exhibit decreased extinction of methamphetamine-conditioned place preference (CPP), as well as increased drug-primed reinstatement of CPP, as compared to controls (Shen et al., 2016). Similarly, adolescent male rats demonstrated increased behavioral sensitization to methamphetamine following prenatal methadone (Wong et al., 2014). The mesolimbic reward circuit has emerged as a key neural substrate on which opioids act to induce changes in behavior. In the nucleus accumbens (NAc), a key target region of dopaminergic inputs from the ventral tegmental area (VTA), endogenous opioids and dopamine facilitate the hedonic and motivational aspects of drug seeking behavior, respectively. The effects of prenatal opioid exposure on the endogenous opioid system have been studied extensively, but much less is known about how prenatal opioid exposure influences the development of the dopamine system with the NAc (Byrnes & Vassoler, 2018). Both dopamine D1 and D2 receptor densities peak in the NAc during adolescence (at approximately postnatal day [P]30) and then decline to adult levels by P55 in the rat (Kopec et al., 2018; Tarazi & Baldessarini, 2000). Microglia, the

resident immune cells of the brain, are increasingly recognized to play a key role in the developmental sculpting of neural circuits. We recently showed that microglial pruning of D1Rs is responsible for this developmental decline following the peak at P30, but only in males (Kopec et al., 2018). Early work has begun to explore the impact of prenatal opioid exposure on microglia. Prenatal methadone exposure reduces the ramification state of microglia in the cortex at P10 (often taken as an indicator of increased proinflammatory activation) and increases brain expression of toll-like receptor 4 (Tlr4) and its adaptor molecule myeloid differentiation primary response protein 88 (MyD88; Jantzie BBI 2020). Furthermore, prenatal exposure to methadone increased serum concentrations of the proinflammatory cytokines interleukin 1ß (IL-1ß), tumor necrosis factor alpha (TNFα), interleukin 6 (Il-6), and the chemokine CXCL1 at P10, and the increase in IL-1ß persisted until P21 (Jantzie BBI 2020).

Based on these collective findings, we hypothesized that prenatal opioid exposure would impact microglial function and alter their pruning of D1rs, leading to persistent alterations in the dopamine system within the NAc, potentially in a sex-specific manner. In line with our hypothesis, our findings demonstrate that microglia engulf less D1R at the peak of pruning, P30, following prenatal opioid exposure, but only in males. Thus, prenatal opioid exposure prevents the developmental decline in NAc-D1R that we previously observed between adolescence and adulthood via altered microglial organization of neural circuits during development.

Methods

Animals

Adult male and female Sprague-Dawley rats (Charles River Laboratory, Wilmington, MA) were group-housed under standard laboratory conditions (12-h light-dark cycle [lights on at 7:00am], food and water ad libitum). All experiments were approved by and conducted in accordance with the Animal Care and Use Committee at McLean Hospital and the National Institutes of Health guide for the care and use of Laboratory animals.

Intravenous oxycodone self-administration

Adult female rats underwent jugular catheter implantation surgery and were trained to self-administer oxycodone prior to mating. Briefly, rats were implanted with chronic, indwelling silastic (0.51mm internal diameter) intravenous jugular catheters as described in Mavrikaki et al., 2017. Catheters were cleaned daily by flushing with 0.2umL of heparinized saline and disinfected once/week with 0.2mL gentamicin (10mg/ml). One week after surgery, females underwent oxycodone self-administration training in operant conditioning chambers (Med Associates, St. Albans, VT, 30.5 x 24.1 x 29.2cm). Operant chambers were enclosed in sound-attenuated cubicles with ventilation fans and contained 2 retractable response levels with cue lights, a house light, a counterbalanced fluid swivel and tether, and an infusion pump. A syringe containing oxycodone solution (0.1mg/kg/infusion) was located outside the chamber and connected to the rat's catheter via a spring-covered Tygon tube connected to a fluid swivel. Upon active lever pressing, rats received a 4 second infusion, the concentration of which was adjusted to the rat's body weight. All rats were given access to self administration for 4hrs/day daily for 5 days. The control group only self-administered for these 5 days. The oxycodone

group continued to self-administer for 7 more days. Next, females in both groups were time-mated, and pregnancy was determined by confirmation of sperm in the vaginal canal (assessed by microscopic evaluation of vaginal swabs). Following mating, the treatment group (oxycodone) continued to self-administer the drug until the day before parturition, while the control group did not. Neither group continued self-administration after parturition.

Neonatal pup outcomes and behavioral quantification

Number of pups in each litter was counted on P1, P3, and P6 to assess neonatal mortality. In addition, milk band size was assessed in all pups as a measure of how much milk they were receiving and categorized according to a 1-4 rating scale (1: no band, 2: small band, 3: medium band, 4: large band). Body weight was also assessed in all offspring at P1, P3, P6 and then again from P21-P50 (P21, P26, P36, P46, P50) to determine long-term changes in weight gain. Neonatal behavioral tests were conducted to assess motor capacities (righting reflex and incline plane). The righting reflex test was conducted at P1 and P3. In this test, pups were flipped onto their back and a stopwatch was used to quantify the number of seconds it took for the pup to right itself. All tests were stopped at 60 sec. Latency to right and the number of pups and percent per litter unable to right were quantified. The inclined plane test was conducted at P6. In this test, pups were placed facing downward on a plane (45° angle) and given 60 sec to turn so that they were facing up the incline rather than down. Pups were scored on the final angle reached (1: 0-90°, 2: 90-179°, 3: 180°) as well on latency to reach 180° (if attained).

Brain Tissue Collection & Sectioning

At P20, P30, and P50, both male and female offspring from both groups were anesthetized using a mixture of ketamine/xylazine and transcardially perfused using ice-cold saline followed by 4% Paraformaldehyde (PFA). Brains were postfixed in 4% PFA for 48 hours followed by 30% sucrose for 48 hours and then frozen at -80°C before cryosectioning at 40µm on a cryostat. Brain sections were stored in cryoprotectant at -20°C until IHC staining. Ages for assessment were chosen based on our previous work (Kopec et al., 2018) to span the adolescent period and to capture the peak timepoint for microglial pruning of D1R (P30).

Immunohistochemistry (IHC)

IHC staining was conducted according to Kopec et al. (2018). Briefly, every 5th section within the NAc was chosen for any given stain (200µm apart). Brain sections were rinsed 5 times in 1xPBS and then incubated at 80°C for 30 min in 10mM sodium citrate (pH 9.0) for epitope retrieval. Next, sections were incubated in 1mg/ml sodium tetraborate in 0.1M PB and then 50% methanol in PBS to quench background fluorescence for 1 hour each. Sections were blocked for 1 hour in 10% goat normal serum with 0.3% Triton-x100 and 3% H202 in 1x PBS before primary antibody incubation. Two separate IHCs were conducted in separate brain sections to label for D1R + microglia (using Iba1) and for dopamine D2 receptor (D2R) and tyrosine hydroxylase (Th; labels dopamine fibers). For D1R and Iba1 staining, sections were incubated for 48 hours at 4°C with a mouse D1R antibody (Novus Biologicals #NB110–60017; Littleton, CO; 1:1500) and a chicken Iba1 antibody (Synaptic Systems, 1:1500). We previously validated the specificity of the Novus D1R antibody in our own hands using D1R knock-out mouse tissue (Kopec et al., 2018). These were followed by secondary antibody incubation with

goat anti-mouse Alexa-Fluor (AF)488 and goat anti-chicken AF568, respectively (Thermofisher Scientific, each 1:500) for 2 hours at room temperature (RT). For D2R and Th staining, sections were incubated for 24 hours at RT with a rabbit D2R antibody (Milllipore, 1:1500) and a mouse Th antibody (Immunostar, 1:1000). These were followed by secondary antibody incubation with goat anti-rabbit AF568 and goat anti-mouse AF488, respectively (both Thermofisher Scientific 1:500). Following IHC, all sections were mounted on gelatin subbed slides, coverslipped with vectashield antifade mounting media with DAPI (Vector Labs), sealed with nail polish, and stored at -20°C until imaging.

Imaging and analysis of D1R, D2R, and Th immunofluorescence

To quantify immunofluorescent intensity in the NAc, 40x magnification Z-stacks were taken on a Zeiss AxioImager microscope. 10 step Z-stacks were taken with a step-size of 0.65µm measured from the center of the focal Z-plane. Images were taken medial to the anterior commissure (AC) using the AC as a landmark. A total of 3-6 images were taken between Bregma +2.76 and +2.28 for each animal (based on the Paxinos and Watson Rat Brain Atlas). For D1R, D2R, and Th, fluorescence intensity in each image was analyzed using FIJI. Briefly, Z-stacks were converted to maximum projection images and mean grey value was measured and normalized to background (defined as the mean grey value of the AC) using the entire images as the ROI. The values of all images taken for a given animal were averaged to provide a single measurement per rat at each age.

IMARIS quantification of microglial engulfment of D1R and microglial morphology

To quantify microglial engulfment of D1R at P30, 63X magnification Z-stacks were taken on a Ziess Airyscan 880 Confocal Laser scanning microscope. Z-stack step size was 0.3 µm and each image had 60-100 steps, aiming to capture entire microglia. Imaris 9.5.1 (Bitplane Scientific Software) was used to create surface renderings of individual microglia (Iba1 labeling) and D1R (D1R labeling) within the microglial surface. Volume of engulfed D1R was then quantified and normalized to total cell volume. 4-5 cells were reconstructed per animal from 3-5 separate brain sections between Bregma distances of +2.76 and +2.28 within the NAc. For assessment of microglial morphology, IMARIS neurite tracer was used to create a skeletonization of individual microglia on which Sholl analyses were conducted.

Statistics

Graphpad Prism version 9.2.1 was used for all statistical analyses. A one-way ANOVA was used to assess self-administration over time in dams. 2-way mixed-effects ANOVAs were (age x treatment) were used to assess number of pups/litter, avg. body weight/litter, body weight per animal, and righting reflex outcomes. Milk band size and inclined plane outcomes were compared using un-paired t-tests. For D1R and Th mean grey values, 2-way ANOVAs (age x treatment) were used, followed by Bonferroni post-hoc tests, in each sex separately because tissues from males and females were processed separately and thus, could be compared directly. For D2R mean grey values at P55, t-tests were used to compare treatment groups. For microglial engulfment analyses, nested t-tests were used to compare treatment groups. For Sholl analyses, nested t-tests were used. All data are represented as mean +/- SEM and significance was set at $p<0.05$.

Results

Prenatal oxycodone exposure impacts neonatal outcomes in offspring

Experimental dams self-administered progressively more oxycodone across pregnancy ($F_{(35,499)}$=1.66, p=0.01, Fig. 1A). In offspring, prenatal opioid exposure significantly decreased the number of surviving pups per litter at P3 and P6 ($F_{(1, 18)}$= 8.66, p<0.01, Fig. 1B, posthoc P3: p<0.01, P6: p<0.01). This is potentially due to impaired nursing, as ~25% of oxycodone pups had no visible milk band and there was a trend towards a smaller proportion of pups that had a milk band classified as medium sized ($t_{(1,18)}$=1.961, p=0.066, Fig. 1C). Average pup body weight per litter was also significantly lower during the perinatal period ($F_{(1,18)}$=7.276, p<0.05, Fig. 1D), and this decrease persisted into adulthood ($F_{(3,131)}$=67.63, p<0.0001, Fig. 1E). Importantly, this persistent decrease in body weight was observed in both males and females (posthoc males: p<0.05, females p<0.001).

The righting reflex and inclined plane tests were conducted at P1 and P3 or P6, respectively (Fig. 2A). We observed only mild effects of prenatal oxycodone treatment on these behavioral outcomes. 45% of oxycodone pups were unable to right themselves within 60 sec. at P1, as compared to 14% of control pups – suggesting motor impairments (Fig. 2B). However, the percentage of pups in each litter that were unable to right in 60 seconds only trended towards significance at P1 ($t_{(1,17)}$=1.528, p=0.14). The average latency to right (per litter) was higher at P1 as compared to P3 (Age effect: $F_{(1,33)}$=4.302, p<0.05, Fig. 2D) but did not differ between treatment groups (Treatment effect: $F_{(1,33)}$=0.689, p=0.413, Fig. 2D). In the inclined plane test, there was no effect of oxycodone on either the final angle reached on average/litter ($t_{(1,14)}$=0.428, p=0.675, Fig. 2E) or on the average latency to reach 180° ($t_{(1,12)}$=0.2064, p=0.95,Fig. 2F).

Prenatal oxycodone exposure increases D1R density in the NAc in adulthood in males but not females

Our previous work showed that D1R density is higher in the NAc at P30 as compared to younger (P20) or older (P55) timepoints in male rats (Kopec et al., 2018). We hypothesized that prenatal oxycodone exposure might prevent the decline in D1R in the NAc between P30 and P55. Thus, we assessed D1R immunofluoresent intensity in the NAc at P20, 30, and 55 (Fig. 3A & B). We found a significant effect of age (p<0.05) and a significant age x treatment interaction effect (p<0.05) for D1R (See Table 1 for complete statistics). Posthoc testing revealed a significant increase in D1R at P55 in oxycodone treated males relative to controls (Fig. 3C&E, p<0.05). Importantly, this increase was male-specific as there was a main effect of age for D1R in the females (Fig. 3F&H, p<0.001), but no treatment or interaction effects. At P55, there was no difference in D2R between control and oxycodone exposed males (Fig. 3D, $t_{(11)}$=0.563; p=0.585) or females (Fig. 3G, $t_{(11)}$=0.536; p=0.602), demonstrating that D1R, but not D2R, is increased in the NAc by prenatal opioid exposure. To determine whether changes in D1R were driven by changes in dopaminergic input to the NAc, we also assessed the density of Th fibers within the NAc at the same timepoints (Fig. 3i). We found significant effects of age in both males (Fig. 3J, p<0.01) and females (Fig. 3K, p<0.001), but no treatment or interaction effects. These findings support our hypothesis that decreased microglial phagocytosis, and not changes

in dopaminergic fiber input to the NAc, is responsible for higher NAc-D1R following prenatal oxycodone exposure.

Prenatal opioid exposure decreases microglial engulfment of NAc-D1R during adolescence in males

We previously showed that microglial complement-dependent phagocytosis of D1R is required for the normal developmental decline in D1R between P30 and P55 in male rats. Moreover, we found that local pharmacological blockade of microglial phagocytosis – specifically at P30 – within the NAc, increased D1R at PD55 (Kopec et al., 2018). Therefore, we hypothesized that higher NAc-D1R following prenatal oxycodone exposure might be due to decreased microglial phagocytosis of D1R at P30 (Fig. 4A). In line with this hypothesis, we found that D1R volume within microglia at P30 was significantly lower following prenatal oxycodone exposure (Fig. 4B&C, % D1R volume/microglia, $t_{(11)}=2.36$; $p<0.05$), while microglia volume did not differ between treatment conditions (Fig. 4D&E, $t_{(11)}=0.97$; $p=0.36$). Interestingly, this effect did not appear to be due to gross changes in microglial morphology, as Sholl analysis revealed no significant differences in number of branch endpoints in microglia (Fig. 4F&G, $t_{(11)}=0.96$; $p=0.39$) or in Schoenen's Ramification Index (Fig. 4H, $t_{(11)}=0.68$; $p=0.51$).

Discussion

Our results demonstrate that prenatal oxycodone exposure increases D1R density in the NAc of young adult male rats (P55) as compared to controls. Notably, this effect is sex-specific as no increase was observed in females. Neither D2R density nor Th-immunoreactive (ir) fiber density in the NAc differed between control and prenatal oxycodone exposed groups, suggesting that higher D1R density is not driven by greater Th inputs to the NAc. Rather, microglial engulfment of D1R is reduced at P30 following prenatal oxycodone exposure in males – a timepoint which we have previously determined is a critical age at which microglia phagocytose NAc-D1Rs (Kopec et al., 2018). Together, these findings suggest that prenatal opioid exposure impairs the ability of microglia to prune D1R during adolescence, thus preventing the normal developmental decline in NAc-D1R between adolescence and adulthood in males only.

Microglia are increasingly recognized to play a critical role in the developmental sculpting of neural circuits in the brain, by phagocytosing synaptic elements and even whole newborn neurons (Faust et al., 2021; Vanryzin et al., 2019). Moreover, human studies have implicated microglia as a key cell type in substance use disorders. For example, RNAsequencing of postmortem brain tissues from individuals with a history of substance use revealed changes in inflammatory gene sets, including TNFα signaling pathways (an important proinflammatory pathway in microglia) specifically within the NAc (Seney et al., 2021). However, virtually nothing is known about how prenatal exposure to drugs of abuse alter microglial phagocytic processes. To our knowledge, our findings are the first demonstration that prenatal opioid exposure disrupts a normal microglial developmental neural circuit pruning program. Indeed, very little work has been done to investigate the impact of prenatal opioid exposure on microglia or neuroimmune function in general. Jantzie et al., (2020) found that perinatal methadone exposure (from embryonic day 16 to P21) increased serum proinflammatory cytokines at P10

including IL-1b, IL-6, TNFa, and CXCL1. Importantly, this increase in circulating IL-1b persisted to P21. They also reported that TLR4 and MyD88 mRNA were elevated in brain tissues from offspring at P10, as were IL-1b and CXCL1 protein. Finally, they found that cortical microglia were rounder with less branch complexity in methadone-exposed offspring as compared to controls at P10 (Jantzie et al., 2020). One important caveat to this work is that the methadone exposure was mostly during the postnatal period, so it is unclear how this is comparable to the prenatal period. For instance, in contrast to Jantzie et al., we did not observe changes in microglial morphology following prenatal opioid exposure. However, it is entirely possible that such a difference could be due to factors such as brain region, type of opioid, and/or age at exposure. Further work is needed to fully characterize the impact of prenatal opioid exposure on microglial function and the relevance of such changes to neural circuit function and behavior.

An outstanding question is how prenatal opioid exposure alters microglial pruning during adolescence. Studies have investigated the molecular pathways by which opioids impact microglial biology in adolescent and adult animals or cell cultures. In adolescent rats, the expression of the chemokines CCL4 and CCL17, as well as their receptor CCR4, are upregulated in microglia isolated from the NAc, following morphine exposure (Schwarz et al., 2013). Moreover, rats that receive repeated morphine during adolescence (but not young adulthood) show persistent changes in microglial function and increased reinstatement to morphine CPP as adults; and, pre-treatment with a glial modulator during adolescent morphine exposure prevents this increased reinstatement, implicating a critical role for microglia (Schwarz et al., 2013), but the precise mechanisms were not defined. In adult male mice, TLR2 is upregulated in the brain by morphine treatment, and TLR2 knock-out (KO) mice have reduced microglial activation in response to morphine (Zhang et al., 2011). Schwarz et al. (2011) found that morphine induces a rapid increase in gene expression for a variety of immune factors within the NAc, including CD11b (i.e. the complement receptor C3R), C-reactive protein, Interferon gamma, CXCL9, CCL11, CCL12, CCL25, CCL17, CCL4, and Ccr4. They also showed that neonatal handling to increase maternal care prevents these increases as well as the reinstatement of morphine CPP. Finally, the protective effect of neonatal handling is mediated by epigenetic programing of the anti-inflammatory cytokine IL-10. Specifically, neonatal handling decreases methylation of the IL-10 gene in microglia – leading to increased IL-10 gene expression in adulthood (Schwarz et al., 2011).

Importantly, none of these studies of opioids and microglia investigated phagocytic processes. However, insight can be gained from literature on peripheral tissue-resident macrophages which share many similarities with microglia. In humans, opioids have been shown to induce immunosuppression in opioid users and, therefore, increased vulnerability to infections, in part by inhibiting macrophage phagocytosis of bacteria (Ninkovic et al., 2016; Kozlowski et al., 2019; Rojavin et al., 1993). Tomassini et al. (2003) found that this opioid inhibition of macrophage phagocytosis appears to be mediated via mu and delta opioid receptor signaling (Tomassini et al., 2003). Similarly, mu opioid knock-out mice do not display opioid-induced reductions in macrophage phagocytosis (Roy et al., 1998). Based on these findings, it is interesting to speculate that mu-opioid receptor signaling might represent a potential mechanism by which down-regulation of microglial D1R phagocytosis is initiated. It

will also be important to investigate the epigenetic programs by which prenatal opioid exposure exerts effects on later-life microglia behavior.

We find that both D1R density and Th-ir fiber density peak in the NAc at P30, in both males and females. These findings are consistent with previous literature showing that D1R peaks in the NAc during adolescence in males (Tarazi & Baldessarini, 2000; Kopec et al., 2018). We extend these findings by showing the Th-ir fiber density follows the same developmental pattern in both males and females. One caveat, however, is that Kopec et al., 2018 found that D1R peaked at P20 in females, rather than at P30. An important difference between that investigation and this one is that control dams in this study were exposed to oxycodone prior to mating and pregnancy. It is possible that this exposure influences the maturation of the dopamine system in females. In line with this idea, studies demonstrate that adolescent morphine exposure prior to pregnancy impacts the development of the opioid system in the next generation of females (Vassoler et al., 2019).

In conclusion, our results provide novel evidence that prenatal opioid exposure disrupts the development of the dopamine system, at least in part by altering microglial engulfment of D1R during adolescence. Importantly, this is only the case in males; no changes in the dopamine system parameters that we assessed were altered by prenatal opioid exposure in females. Further work is needed to shed light on the molecular mechanisms by which these changes occur, as well as their long-term implications for behavior. Finally, the factors that provide resilience in the face of opioid exposure in females remain to be elucidated.

Bibliography

Abu, Y., & Roy, S. (2021). Prenatal opioid exposure and vulnerability to future substance use disorders in offspring. Experimental Neurology, 339, 113621.

Arter, S., Lambert, J., Brokman, A., & Fall, N. (2021). Diagnoses during the first three years of life for children with prenatal opioid exposure and neonatal abstinence syndrome using a large maternal infant data hub. Journal of Pediatric Nursing, 61, 34–39.

Benninger, K. L., Borghese, T., Kovalcik, J. B., Moore-Clingenpeel, M., Isler, C., Bonachea, E. M., Stark, A. R., Patrick, S. W., & Maitre, N. L. (2020). Prenatal Exposures Are Associated With Worse Neurodevelopmental Outcomes in Infants With Neonatal Opioid Withdrawal Syndrome. Frontiers in Pediatrics, 8, 462.

Boggess, T., & Risher, W. C. (2020). Clinical and basic research investigations into the long-term effects of prenatal opioid exposure on brain development. Journal of Neuroscience Research. https://doi.org/10.1002/jnr.24642

Byrnes, E. M., & Vassoler, F. M. (2018). Modeling prenatal opioid exposure in animals: Current findings and future directions. Frontiers in Neuroendocrinology, 51, 1–13.

Conradt, E., Flannery, T., Aschner, J. L., Annett, R. D., Croen, L. A., Duarte, C. S., Friedman, A. M., Guille, C., Hedderson, M. M., Hofheimer, J. A., Jones, M. R., Ladd-Acosta, C., McGrath, M., Moreland, A., Neiderhiser, J. M., Nguyen, R. H. N., Posner, J., Ross, J. L., Savitz, D. A., … Lester, B. M. (2019). Prenatal Opioid Exposure: Neurodevelopmental Consequences and Future Research Priorities. Pediatrics, 144(3). https://doi.org/10.1542/peds.2019-0128

de Cubas, M. M., & Field, T. (1993). Children of methadone-dependent women: developmental outcomes. The American Journal of Orthopsychiatry, 63(2), 266–276.

Faust, T. E., Gunner, G., & Schafer, D. P. (2021). Mechanisms governing activity-dependent synaptic pruning in the developing mammalian CNS. Nature Reviews. Neuroscience, 22(11), 657–673.

Haight, S. C., Ko, J. Y., Tong, V. T., Bohm, M. K., & Callaghan, W. M. (2018). Opioid Use Disorder Documented at Delivery Hospitalization - United States, 1999-2014. MMWR. Morbidity and Mortality Weekly Report, 67(31), 845–849.

Hunt, R. W., Tzioumi, D., Collins, E., & Jeffery, H. E. (2008). Adverse neurodevelopmental outcome of infants exposed to opiate in-utero. Early Human Development, 84(1), 29–35.

Jantzie, L. L., Maxwell, J. R., Newville, J. C., Yellowhair, T. R., Kitase, Y., Madurai, N., Ramachandra, S., Bakhireva, L. N., Northington, F. J., Gerner, G., Tekes, A., Milio, L. A., Brigman,

J. L., Robinson, S., & Allan, A. (2020). Prenatal opioid exposure: The next neonatal neuroinflammatory disease. Brain, Behavior, and Immunity, 84, 45–58.

Kopec, A. M., Smith, C. J., Ayre, N. R., Sweat, S. C., & Bilbo, S. D. (2018). Microglial dopamine receptor elimination defines sex-specific nucleus accumbens development and social behavior in adolescent rats. Nature Communications, 9(1), 3769.

Kozlowski, M., Nazimek, K., Nowak, B., Filipczak-Bryniarska, I., & Bryniarski, K. (2019). Analgesic adjuvants modulate morphine-induced immune effects in mice. Pharmacological Reports: PR, 71(4), 573–582.

Mavrikaki, M., Pravetoni, M., Page, S., Potter, D., & Chartoff, E. (2017). Oxycodone self-administration in male and female rats. Psychopharmacology, 234(6), 977–987.

Moe, V. (2002). Foster-placed and adopted children exposed in utero to opiates and other substances: prediction and outcome at four and a half years. Journal of Developmental and Behavioral Pediatrics: JDBP, 23(5), 330–339.

Ninković, J., & Roy, S. (2012). Morphine decreases bacterial phagocytosis by inhibiting actin polymerization through cAMP-, Rac-1-, and p38 MAPK-dependent mechanisms. The American Journal of Pathology, 180(3), 1068–1079.

Nygaard, E., Moe, V., Slinning, K., & Walhovd, K. B. (2015). Longitudinal cognitive development of children born to mothers with opioid and polysubstance use. Pediatric Research, 78(3), 330–335.

Nygaard, E., Slinning, K., Moe, V., & Walhovd, K. B. (2017). Cognitive function of youths born to mothers with opioid and poly-substance abuse problems during pregnancy. Child Neuropsychology: A Journal on Normal and Abnormal Development in Childhood and Adolescence, 23(2), 159–187.

Rojavin, M., Szabo, I., Bussiere, J. L., Rogers, T. J., Adler, M. W., & Eisenstein, T. K. (1993). Morphine treatment in vitro or in vivo decreases phagocytic functions of murine macrophages. Life Sciences, 53(12), 997–1006.

Roy, S., Barke, R. A., & Loh, H. H. (1998). MU-opioid receptor-knockout mice: role of mu-opioid receptor in morphine mediated immune functions. Brain Research. Molecular Brain Research, 61(1-2), 190–194.

Sandtorv, L. B., Fevang, S. K. E., Nilsen, S. A., Bøe, T., Gjestad, R., Haugland, S., & Elgen, I. B. (2018). Symptoms Associated With Attention Deficit/Hyperactivity Disorder and Autism Spectrum Disorders in School-Aged Children Prenatally Exposed to Substances. Substance Abuse: Research and Treatment, 12, 1178221818765773.

Schwarz, J. M., & Bilbo, S. D. (2013). Adolescent morphine exposure affects long-term microglial function and later-life relapse liability in a model of addiction. The Journal of Neuroscience: The Official Journal of the Society for Neuroscience, 33(3), 961–971.

Schwarz, J. M., Hutchinson, M. R., & Bilbo, S. D. (2011). Early-life experience decreases drug-induced reinstatement of morphine CPP in adulthood via microglial-specific epigenetic programming of anti-inflammatory IL-10 expression. The Journal of Neuroscience: The Official Journal of the Society for Neuroscience, 31(49), 17835–17847.

Schwarz, J. M., Smith, S. H., & Bilbo, S. D. (2013). FACS analysis of neuronal-glial interactions in the nucleus accumbens following morphine administration. Psychopharmacology, 230(4), 525–535.

Seney, M. L., Kim, S.-M., Glausier, J. R., Hildebrand, M. A., Xue, X., Zong, W., Wang, J., Shelton, M. A., Phan, B. N., Srinivasan, C., Pfenning, A. R., Tseng, G. C., Lewis, D. A., Freyberg, Z., & Logan, R. W. (2021). Transcriptional Alterations in Dorsolateral Prefrontal Cortex and Nucleus Accumbens Implicate Neuroinflammation and Synaptic Remodeling in Opioid Use Disorder. Biological Psychiatry, 90(8), 550–562.

Shen, Y.-L., Chen, S.-T., Chan, T.-Y., Hung, T.-W., Tao, P.-L., Liao, R.-M., Chan, M.-H., & Chen, H.-H. (2016). Delayed extinction and stronger drug-primed reinstatement of methamphetamine seeking in rats prenatally exposed to morphine. Neurobiology of Learning and Memory, 128, 56–64.

Singer, L. T., Chambers, C., Coles, C., & Kable, J. (2020). Fifty Years of Research on Prenatal Substances: Lessons Learned for the Opioid Epidemic. Adversity and Resilience Science, 1(4), 223–234.

Skumlien, M., Ibsen, I. O., Kesmodel, U. S., & Nygaard, E. (2020). Sex Differences in Early Cognitive Development After Prenatal Exposure to Opioids. Journal of Pediatric Psychology, 45(5), 475–485.

Tarazi, F. I., & Baldessarini, R. J. (2000). Comparative postnatal development of dopamine D(1), D(2) and D(4) receptors in rat forebrain. International Journal of Developmental Neuroscience: The Official Journal of the International Society for Developmental Neuroscience, 18(1), 29–37.

Tomassini, N., Renaud, F. L., Roy, S., & Loh, H. H. (2003). Mu and delta receptors mediate morphine effects on phagocytosis by murine peritoneal macrophages. Journal of Neuroimmunology, 136(1-2), 9–16.

van Baar, A., & de Graaff, B. M. (1994). Cognitive development at preschool-age of infants of drug-dependent mothers. Developmental Medicine and Child Neurology, 36(12), 1063–1075.

VanRyzin, J. W., Marquardt, A. E., Argue, K. J., Vecchiarelli, H. A., Ashton, S. E., Arambula, S. E., Hill, M. N., & McCarthy, M. M. (2019). Microglial Phagocytosis of Newborn Cells Is Induced by Endocannabinoids and Sculpts Sex Differences in Juvenile Rat Social Play. Neuron, 102(2), 435–449.e6.

Vassoler, F. M., Toorie, A. M., & Byrnes, E. M. (2019). Multi-, Inter-, and Transgenerational Effects of Drugs of Abuse on Behavior. Current Topics in Behavioral Neurosciences, 42, 247–258.

Wong, C.-S., Lee, Y.-J., Chiang, Y.-C., Fan, L.-W., Ho, I.-K., & Tien, L.-T. (2014). Effect of prenatal methadone on reinstated behavioral sensitization induced by methamphetamine in adolescent rats. Behavioural Brain Research, 258, 160–165.

Zhang, Y., Li, H., Li, Y., Sun, X., Zhu, M., Hanley, G., Lesage, G., & Yin, D. (2011). Essential role of toll-like receptor 2 in morphine-induced microglia activation in mice. Neuroscience Letters, 489(1), 43–47.

Figure Legends

Figure 1. Prenatal opioid exposure impacts neonatal outcomes in offspring. A) Rat dams self administered oxycodone for either 5 days pre-pregnancy (Controls) or throughout gestation. **B**) Number of pups per litter was significantly decreased at P3 and P6 following oxycodone exposure. **C**) ~ 20% of oxytocodone exposed pups lacked a detectable milk band and oxycodone pups tended to have fewer medium-size milk bands. **D**) We observed a main effect of treatment such that the average body weight of oxycodone exposed litters was smaller than that of control litters. **E**) Both male and female oxycodone exposed offspring were persistently lower in body weight into adulthood. A-D: N = 7 litters (CON), 12 litters (Oxycodone), male and female offspring are combined. Data represent Mean +/- SEM, *p=0.05.

Figure 2. Prenatal opioid exposure does not persistently impact neonatal motor behaviors. A) Schematic of timeline for behavioral tests. **B**) 46% of oxycodone exposed pups were unable to right themselves in 60 sec. on P1, as compared to only 14% of control pups, N=79-127 pups per group. **C**) There was no significant treatment effect on the % of each litter unable to right or on the latency to right (**D**), N (litters) = 6 (P1 control), 5 (P3 control), 13 (P1 oxycodone), 12 (P3 oxycodone). However, both measures were significantly lower at P3 as compared to P1. **E**) There was no difference between control and oxycodone pups in the final angle reached in the inclined plane test, or in the latency to reach 180° (**F**). Data represent Mean +/- SEM, *p=0.05.

Figure 3. Prenatal oxycodone exposure increases D1R density in the NAc in adulthood in males but not females. A) Schematic of timeline for treatment and tissue collection. **B**) Rat brain atlas images delineating NAc region where D1R, D2R, and Th were quantified (based on Paxinos and Watson Rat Brain Atlas). **C**) In males, D1R mean grey value differed significantly with age, and was higher at P55 in oxycodone exposed males as compared to control. **D**) D2R did not differ with treatment at P55 in males. **E**) Representative 20x images of D1R staining in the NAc of males, scale bar= 27 microns. **F**) D1R peaked at P30 in both control and oxycodone exposed females, but did not differ with treatment. **G**) D2R did not differ with treatment at P55 in females. **H**) Representative 20x images of D1R staining in the NAc of females, scale bar= 27 microns. **I**) Representative 20 image of Th staining in the NAc of males, scale bar = 27 microns. **J**) Th peaked at P30 in both control and oxycodone exposed males and females (**K**), but did not differ with treatment. Data represent Mean +/- SEM, *p=0.05.

Figure 4. Prenatal opioid exposure decreases microglial engulfment of NAc-D1R during adolescence in males. A) Schematic of timeline for exposures and P30 engulfment assessment. B) D1R volume within microglia was significantly decreased following oxycodone exposure in male offspring at P30. C) % D1R volume of total microglial volume was significantly decreased following oxycodone exposure in male offspring at P30. D) There was no treatment effect on microglial volume. E) Representative 60X images of microglial D1R engulment: grey: Iba1, green: D1R, scale bar= 5 microns. F) Scholl analysis revealed no differences in # of intersections between control and oxycodone males, or in branch endpoints (G) or Ramification Index (H). B-

H: dots represent individual microglia, N=29 (control), 30 (oxycodone) nested per animal 6 and 7, respectively for analysis (nested t-tests). Data represent Mean +/- SEM, *p=0.05.

Table 1. Complete results of 2-way ANOVAs (treatment x age) for D1R and Th in male and female offspring with Bonferroni posthoc tests. Values represent p values, bolded if significant at p<0.05. Color coding indicates significant age comparisons (blue) and treatment comparisons (green).

Comparison:	**D1R Males**	**Th Males**	**D1R Females**	**Th Females**
Main effect: Treatment	**$F_{(1, 30)}$ = 9.766, p=0.004**	$F_{(1, 29)}$ = 0.752, p=0.752	$F_{(1, 32)}$ = 0.309, p=0.582	$F_{(1, 32)}$ = 0.379, p=0.542
Main effect: Age	**$F_{(2, 30)}$ = 3.983, p=0.029**	**$F_{(2, 29)}$ = 6.500, p=0.005**	**$F_{(2,32)}$ = 10.83, p<0.001**	**$F_{(2,32)}$ = 9.090, p<0.001**
Interaction Effect: Treatment x Age	$F_{(2,30)}$ = 2.265, p=0.121	$F_{(2, 29)}$ = 0.941, p=0.402	$F_{(2,32)}$ = 2.166, p=0.131	$F_{(2,32)}$ = 0.680, p=0.514
Posthoc PD20 vs PD30	**p=0.031**	**p=0.041**	**p<0.001**	**p=0.001**
Posthoc PD30 vs PD55	p>0.999	**p=0.006**	**p<0.001**	**p=0.007**
Posthoc PD20 vs PD55	p=0.155	p>0.999	p>0.999	p>0.999
Posthoc Control vs. Oxycodone PD20	p>0.999	p>0.999	p=0.963	p>0.999
Posthoc Control vs. Oxycodone PD30	p=0.897	p>0.999	p=0.201	p=0.676
Posthoc Control vs. Oxycodone PD55	**p=0.003**	p=0.675	p>0.999	p>0.999

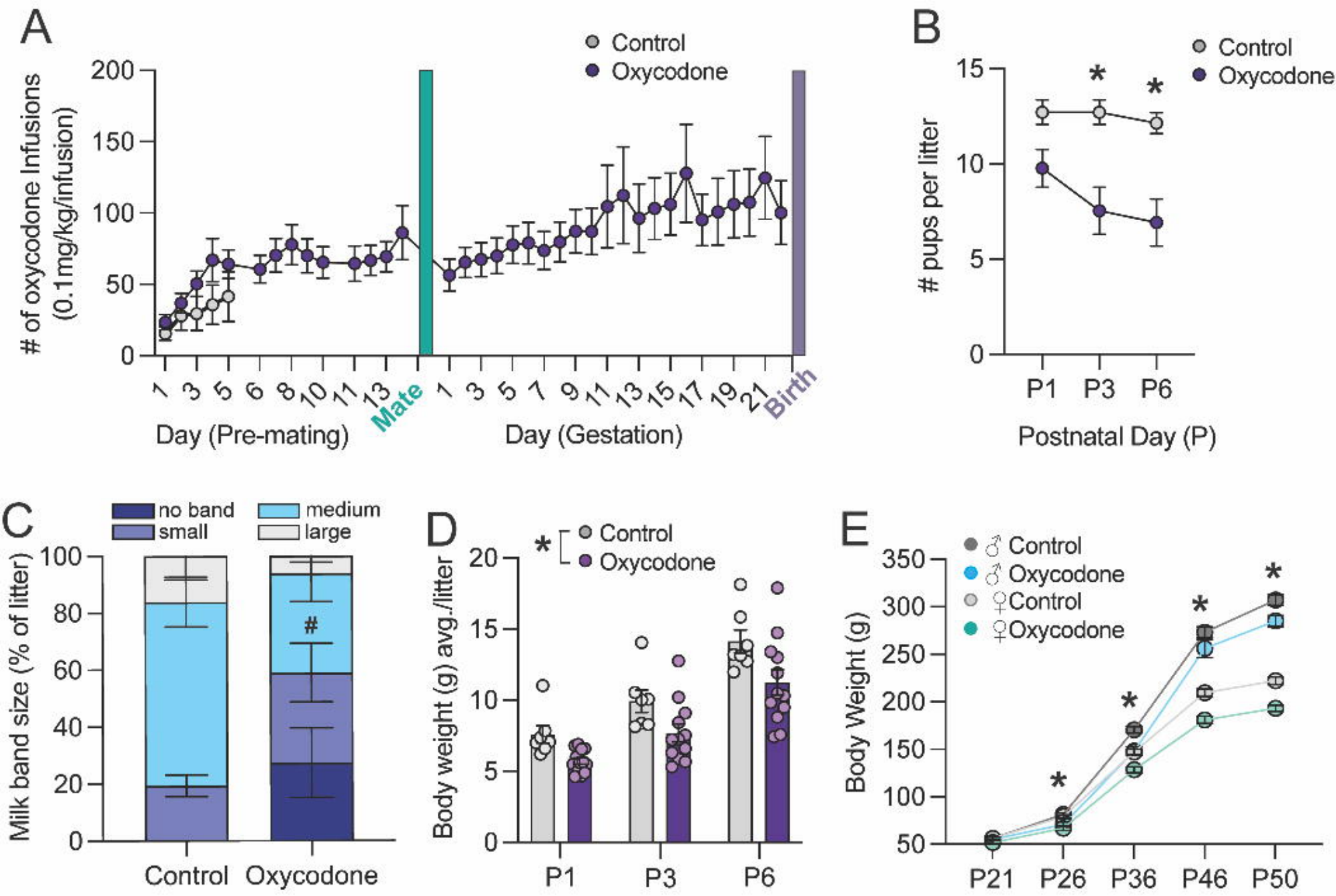
A
Control
Oxycodone
# of oxycodone Infusions
(0.1mg/kg/infusion)
200
150
100
50
0
1 3 5 6 8 10 11 13
Mate
1 3 5 7 9 11 13 15 17 19 21
Birth
Day (Pre-mating)
Day (Gestation)
B
Control
Oxycodone
pups per litter
15
10
5
0
*
*
P1 P3 P6
Postnatal Day (P)
C
no band
small
medium
large
Milk band size (% of litter)
100
80
60
40
20
0
#
Control
Oxycodone
D
Control
Oxycodone
*
Body weight (g) avg./litter
20
15
10
5
0
P1
P3
P6
E
♂ Control
♂ Oxycodone
♀ Control
♀ Oxycodone
Body Weight (g)
350
300
250
200
150
100
50
*
*
*
*
P21
P26
P36
P46
P50

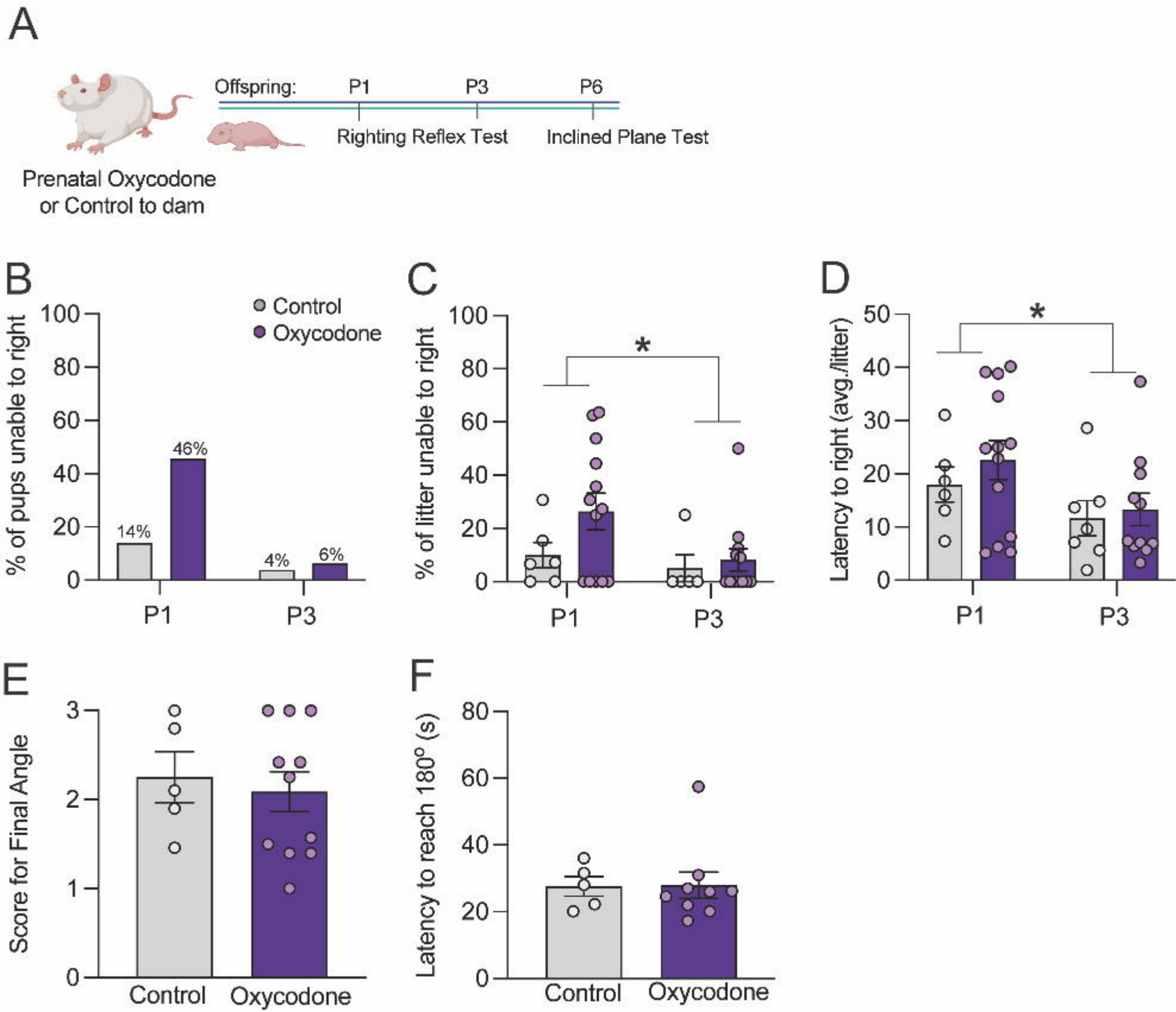
A
Offspring:
P1
P3
P6
Righting Reflex Test
Inclined Plane Test
Prenatal Oxycodone
or Control to dam
B
Control
Oxycodone
% of pups unable to right
100
80
60
40
20
0
46%
14%
4%
6%
P1
P3
C
% of litter unable to right
*
D
Latency to right (avg./litter)
50
40
30
20
10
E
Score for Final Angle
3
2
1
Control
Oxycodone
F
Latency to reach 180° (s)
80
60

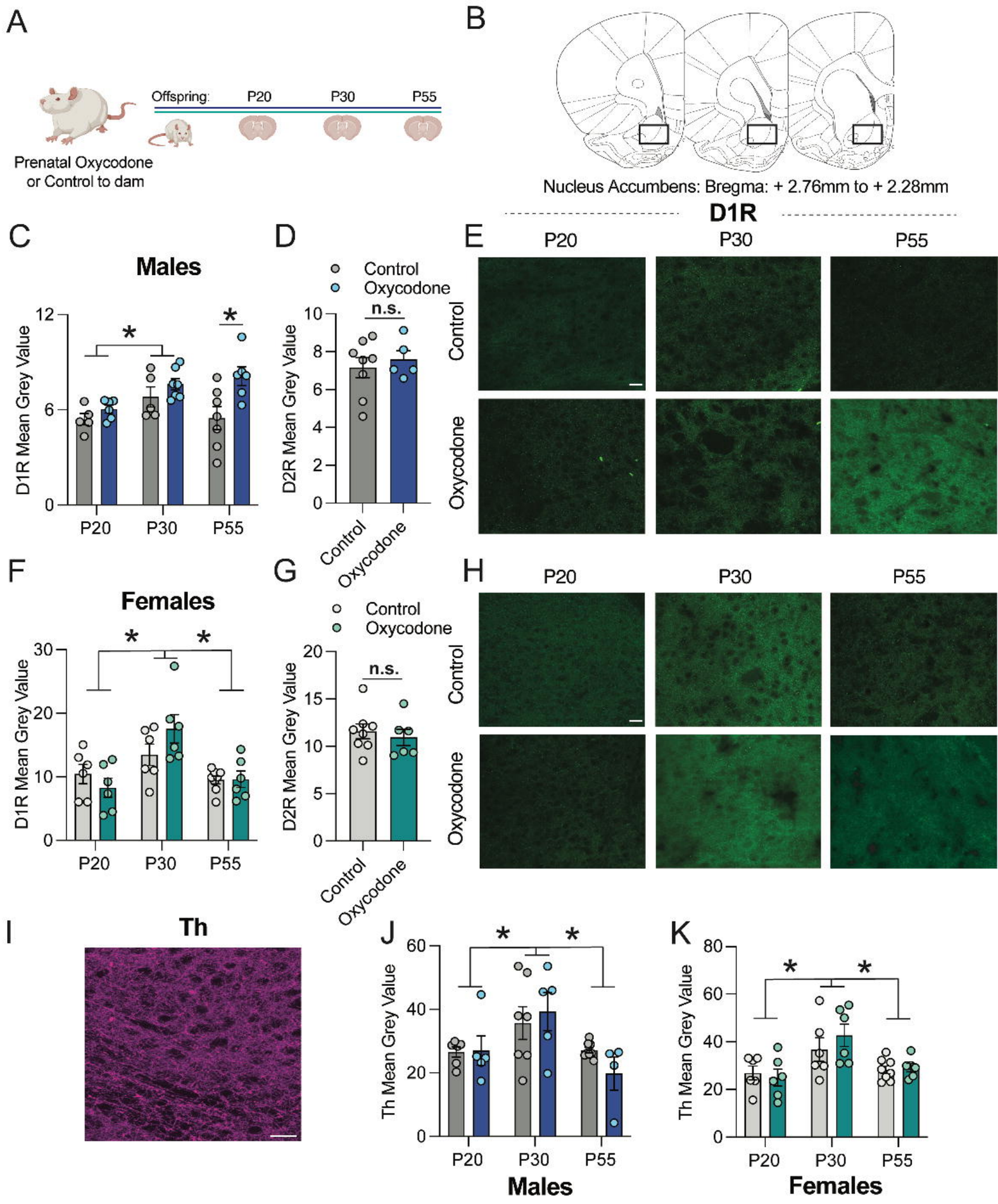
A
Offspring:
P20
P30
P55
Prenatal Oxycodone
or Control to dam
B
Nucleus Accumbens: Bregma: + 2.76mm to + 2.28mm
D1R
C
Males
D1R Mean Grey Value
P20
P30
P55
D
Control
Oxycodone
n.s.
D2R Mean Grey Value
E
P20
P30
P55
Control
Oxycodone
F
Females
G
H
I
Th
J
Th Mean Grey Value
Males
K
Females

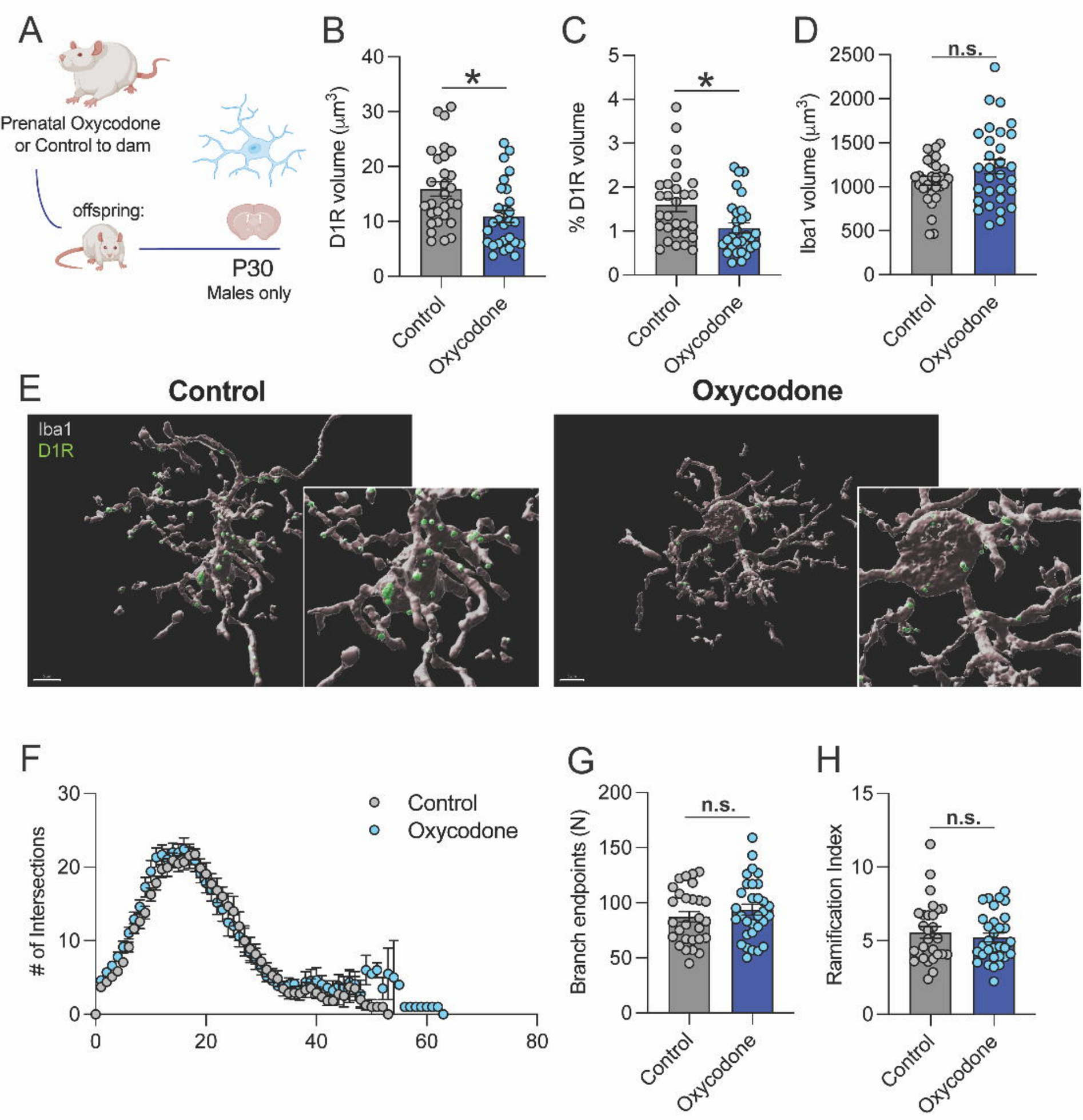
A
Prenatal Oxycodone
or Control to dam
offspring:
P30
Males only
B
D1R volume (μm3)
Control
Oxycodone
C
% D1R volume
Control
Oxycodone
D
Iba1 volume (μm3)
n.s.
Control
Oxycodone
E
Control
Oxycodone
Iba1
D1R
F
# of Intersections
Control
Oxycodone
G
Branch endpoints (N)
n.s.
Control
Oxycodone
H
Ramification Index
n.s.
Control
Oxycodone